Narrowing of the neutron *sd*-*pf* shell gap in ^{29}Na

A. M. Hurst [a,*], C. Y. Wu [a], J. A. Becker [a], M. A. Stoyer [a], C. J. Pearson [b], G. Hackman [b], M. A. Schumaker [c], C. E. Svensson [c], R. A. E. Austin [d], G. C. Ball [b], D. Bandyopadhyay [b], C. J. Barton [e], A. J. Boston [f], H. C. Boston [f], R. Churchman [b], D. Cline [g], S. J. Colosimo [d], D. S. Cross [h], G. Demand [c], M. Djongolov [b], T. E. Drake [i], P. E. Garrett [c], C. Gray-Jones [f], K. L. Green [c], A. N. Grint [f], A. B. Hayes [g], K. G. Leach [c], W. D. Kulp [j], G. Lee [b], S. Lloyd [b], R. Maharaj [b], J-P. Martin [k], B. A. Millar [c], S. Mythili [ℓ], L. Nelson [f], P. J. Nolan [f], D. C. Oxley [f], E. Padilla-Rodal [b], A. A. Phillips [c], M. Porter-Peden [m], S. V. Rigby [f], F. Sarazin [m], C. S. Sumithrarachchi [c], S. Triambak [c], P. M. Walker [n], S. J. Williams [b], J. Wong [c], J. L. Wood [j]

[a] *Lawrence Livermore National Laboratory, Livermore, California 94550, USA*

[b] *TRIUMF, 4004 Westbrook Mall, Vancouver BC, V6T 2A3, Canada*

[c] *Department of Physics, University of Guelph, Guelph ON, N1G 2W1, Canada*

[d] *Department of Astronomy and Physics, Saint Mary's University, Halifax NS, B3H 3C3, Canada*

[e] *Department of Physics, University of York, York YO10 5DD, United Kingdom*

[f] *Oliver Lodge Laboratory, University of Liverpool, Liverpool L69 7ZE, United Kingdom*

[g] *Department of Physics and Astronomy, University of Rochester, Rochester, NY 14627, USA*

[h] *Department of Chemistry, Simon Fraser University, Burnaby BC, V5A 1S6, Canada*

[i] *Department of Physics, University of Toronto, Toronto ON, M5S 1A7, Canada*

[j] *School of Physics, Georgia Institute of Technology, Atlanta, Georgia 30332, USA*

[k] *Department of Physics, University of Montreal, Montreal QC, G1K 7P4, Canada*

[ℓ] *Department of Physics, University of British Columbia, Vancouver BC, V6T 1Z1, Canada*

[m] *Physics Department, Colorado School of Mines, Golden, Colorado 80401, USA*

[n] *Department of Physics, University of Surrey, Guildford, Surrey GU2 7XH,*

Preprint submitted to Elsevier *16 January 2009*

United Kingdom

Abstract

The wave-function composition for the low-lying states in ^{29}Na was explored by measuring their electromagnetic properties using the Coulomb-excitation technique. A beam of ^{29}Na ions, postaccelerated to 70 MeV, bombarded a ^{110}Pd target with a rate of up to 600 particles per second at the recently commissioned ISAC-II facility at TRIUMF. Six segmented HPGe clover detectors of the TIGRESS γ-ray spectrometer were used to detect deexcitation γ rays in coincidence with scattered or recoiling charged particles in the segmented silicon detector, BAMBINO. The reduced transition matrix element $|\langle \frac{5}{2}^{+}_{1} || E2 || \frac{3}{2}^{+}_{\rm gs} \rangle|$ in ^{29}Na was derived to be 0.237(21) eb from the measured γ-ray yields for both projectile and target. This first-time measured value is consistent with the most recent Monte Carlo shell-model calculation, indicating a significant admixture of both *sd* and *pf* components in the wave function, and also providing evidence for the narrowing of the *sd*-*pf* shell gap from ~ 6 MeV for stable nuclei to ~ 3 MeV for ^{29}Na.

Key words: Coulomb excitation, ISOL, reduced transition matrix element, island of inversion
PACS: 21.10.Ky, 23.40.Hc, 25.70.De, 27.30.+t

The success of the shell model applied to atomic nuclei derives its origins from the existence of a set of "magic" numbers [1,2] corresponding to particularly stable proton and neutron configurations in nuclei along, or close to, the line of β stability. However, it has since come to light that these magic numbers are not universal quantities, and for certain exotic nuclei new magic numbers appear while the established ones disappear. The physical origin of this phenomenon may be attributed to the isospin-dependent part of the nucleon-nucleon interaction in nuclei [3–5]. Probing the effective nuclear interaction in exotic nuclei, belonging to regions of the nuclear landscape where the neutron/proton ratio is significantly different than near stability, will thus provide important new information to challenge current theoretical predictive capabilities.

For neutron-rich light nuclei with $Z \sim 12$ and $N \sim 20$, a region far from stability, the protons occupy the $d_{5/2}$ orbits at the bottom of the *sd* shell whereas the neutrons−at least in the traditional shell model picture−are expected to populate the $d_{3/2}$ orbitals up to the $N = 20$ shell-model magic number. However, for some of these neutron-rich nuclei it has already been demonstrated that the valence neutrons begin to fill the lower orbits of the

* Corresponding author.
Email address: hurst10@llnl.gov (A. M. Hurst).

next major shell, the pf shell, before completely filling the $d_{3/2}$ orbit of the sd shell [6,7]. It is therefore important to experimentally study this evolution along a given isotope chain to provide essential data for modeling the effective nuclear interaction in nuclei across the entire nuclear chart.

Early experimental and theoretical investigations into the properties of these neutron-rich nuclei resulted in the identification of Na [8,9], and Mg [10,11] nuclei with binding energies and other structural characteristics that could not be explained on the basis of pure sd configurations [12]. Outlying nuclei were identified through a comparison of measured nuclear properties with predictions of large-scale shell model calculations using the universal sd-shell (USD) effective interaction [13]; an effective interaction that has achieved remarkable success in predicting properties of sd-shell nuclei. The properties of the Na nuclei illustrate the case. Stable ^{23}Na with $N/Z = 1.1$ is very well described within the sd framework by the USD effective interaction. The USD description of the Na nuclei remains valid with increasing neutron number for ^{28}Na ($N/Z = 1.5$) but not necessarily for ^{29}Na ($N/Z = 1.6$). The β-decay studies of Tripathi *et al.* [14,15] show that ^{29}Na is not well described by USD calculations, however this interpretation is complicated by a possible 2p-2h intruder component in the ground state of ^{29}Ne [16]. Furthermore the experimentally determined ground-state quadrupole moment for ^{29}Na [17] is ~ 30 % larger than predicted by the USD. The addition of one more neutron in ^{30}Na reveals a collective structure [18–20], quite unlike the expected single-particle characterisation based on three protons in the $d_{3/2}$ orbital. This intriguing scenario may be explained by assuming that the last few valence neutrons do not fill the expected orbitals in accordance with standard shell-model ordering near stability, but rather jump to the lower orbitals of the next major pf shell [20]. Such a phenomenon implies that the sd-pf shell gap narrows in ^{29}Na to an extent that the energetics are beginning to favour population of the pf shell, even though the $N = 20$ shell closure is not complete. Complex shell-model calculations performed using effective Hamiltonians incorporating the sd and pf shell-model spaces, including the cross-shell mixing terms, support this hypothesis [20–22]. The most recent calculation of ^{29}Na utilising Monte Carlo shell-model (MCSM) techniques with an SDPF-M Hamiltonian [20], based on a valence shell comprising all the sd-shell orbits and the two lower orbits of the pf shell and with the effective charges $(e_p, e_n) = (1.3e, 0.5e)$, predicts strong mixing between the sd and pf shells at ^{29}Na ($N = 18$), while ^{28}Na is predicted to have a nearly pure 0p-0h normal sd configuration, and ^{30}Na a nearly pure 2p-2h intruder pf configuration. The $f_{7/2}p_{3/2}$ wave-function admixtures imply that significant collectivity develops for electromagnetic transitions between the low-lying positive parity states in ^{29}Na.

This work tests these predictions for the boundary nucleus ^{29}Na using sub-barrier Coulomb excitation to excite the 72-keV first-excited state in this nucleus and determine the $E2$ matrix element for its decay. In this Letter

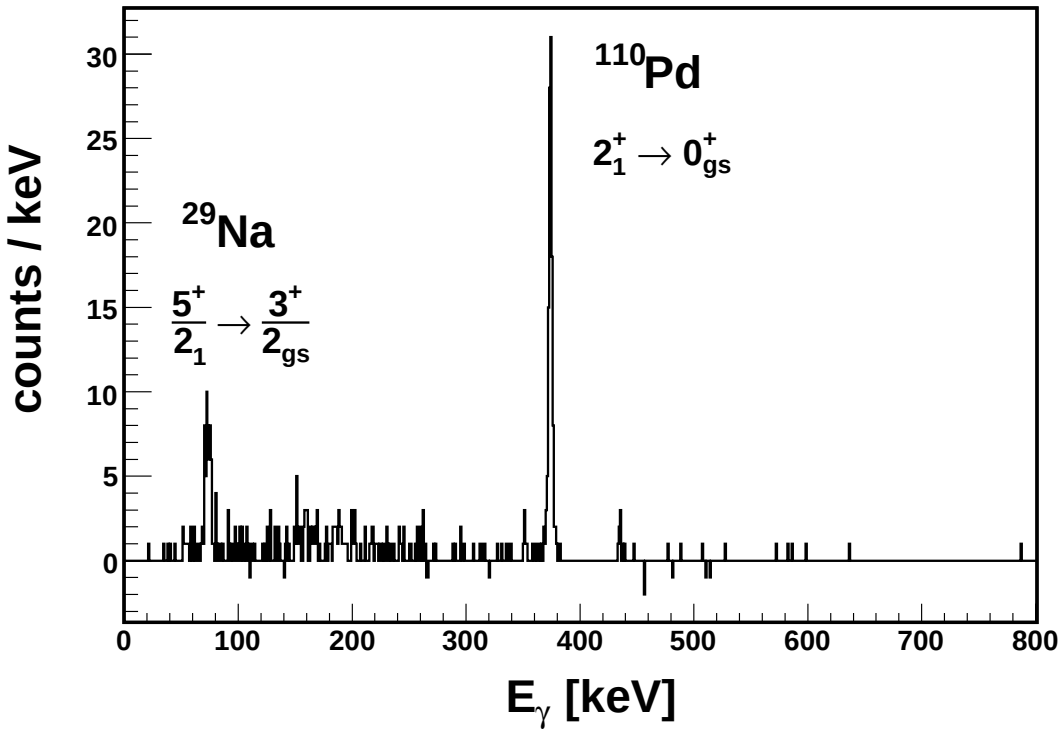

Fig. 1. Particle-γ coincident, suppressed, random-subtracted γ-ray energy spectrum observed following $\sim$ 70 h of beam on target corresponding to ^{110}Pd(^{29}Na,^{29}Na*) at $E_{\rm beam}$ = 70 MeV. The prominent peaks are marked and correspond to the $5/2_1^+ \rightarrow 3/2_{\rm gs}^+$ transition at 72 keV in ^{29}Na, and the $2_1^+ \rightarrow 0_{\rm gs}^+$ at 374 keV in ^{110}Pd.

we report the first measurement of the reduced transition matrix element $\langle \frac{5}{2}^+_1 || E2 || \frac{3}{2}^+_{\rm gs} \rangle$ for ^{29}Na.

The energetic beam of ^{29}Na was obtained by fragmentation in a Ta primary target bombarded by a 500-MeV, 70-μA proton beam at the TRIUMF cyclotron. The ^{29}Na atoms effusing out of the target were ionised to singly-charged ^{29}Na$^+$ in a Re surface-ion source, accelerated to 58 kV, then separated according to A/q in a magnetic sector field and transported to an RFQ where they were accelerated to $150 \cdot A$ keV. The delivery of a high-quality radioactive ^{29}Na$^+$ beam was enabled through tuning efforts with a stable ^{58}Ni^{2+} pilot beam, both species having $A/q = 29$. The ^{29}Na$^+$ ions were subsequently stripped to ^{29}Na^{5+} ions ($A/q = 5.8$) and postaccelerated to $1.53 \cdot A$ MeV by the room-temperature Drift Tube LINAC, ISAC-I [23]. Surviving ions were transported to the superconducting LINAC components of ISAC-II [23,24] via an achromatic S-bend transfer line, accelerated to final total bombarding energy of 70 MeV, and delivered to a secondary Coulomb-excitation target comprising a 2.94-mg/cm^2 foil of ^{110}Pd (97.6 % enriched) with a beam intensity as large as 600 ions/s. Six Compton-suppressed clovers of the TIGRESS array [25] were arranged around the target chamber. Each clover comprises 32-fold segmented HPGe detectors coupled with 12-fold segmented modular Compton

suppression shields. The faces of the clover detectors were 11 cm from the target while these detectors subtended a polar laboratory range from 22.5° to 157.5°, covering approximately 36 % of 4π. An annular double-sided 140-μm thick silicon detector, BAMBINO, was mounted 3 cm downstream of the target position, perpendicular to the beam direction, and was used for detection of the scattered beam and recoiling target particles. The front face of BAMBINO is segmented into 32 sector strips, while the back face is composed of 24 annular strips. This detector covered a range of forward laboratory angles between 20.1° and 49.4°. The $A = 29$ beam was dumped in a beam-stopper ~ 1 m downstream of the Coulomb-excitation target. Spectra from an 80 % HPGe detector at this position only revealed γ-decay lines belonging to the subsequent β^--decay products of ^{29}Na ($T_{\frac{1}{2}} = 44.9(12)$ ms).

Although it is possible to kinematically distinguish the projectile- and target-like particles through their energy as a function of the laboratory angle, in order to maximise statistics from this low event-rate experiment, the coincidence γ-ray energy spectrum presented in Fig. 1 was generated according to acceptance of either particle type impinging onto BAMBINO and thus corresponds to acceptance of both particle types arriving within the prompt-coincident event window. A wide prompt particle-γ coincidence window of ~ 700 ns was used to ensure that all low-energy ^{29}Na events were accounted for with full efficiency.

Isobaric contamination of the incident beam is often a prevalent issue and must be investigated thoroughly in radioactive-beam experiments. The particle-energy spectrum shown in Fig. 2 corresponds to the total energy deposited in the two innermost rings of BAMBINO (covering an angular range from 20.1° to 23.4°) and reveals two sharp peaks centered around 45 MeV and 50 MeV indicating a two-component beam mixture. With energy loss considerations (both in the ^{110}Pd target as well as the 0.58-mg/cm^2 thick ^{197}Au coating on the silicon strips) particle-energy peaks at 45 MeV and 50 MeV were assigned to scattered particles corresponding to ^{29}Al and ^{29}Na, respectively. The ^{110}Pd-target recoils can be identified by the broad peak at low energy in the spectrum. The $A = 29$ beam was by composition 72.0(8) % ^{29}Na and 28.0(8) % ^{29}Al, determined from this energy spectrum and the calculated Rutherford cross sections integrated over the energy losses of the isobars in the target and the total polar range subtended by the two annular strips.

Excitation of both projectile and target was observed in this experiment due to the electromagnetic interaction between the colliding nuclei. Since the average projectile-target surface distance was always greater than 5 fm at the incident bombarding energy, any nuclear interference is therefore considered negligible [26]. Under these conditions, only the lowest-lying excited state is expected to be strongly populated in each nucleus, with excitations to higher states significantly weaker, ~ 1 % or less. Determination of the transition ma-

trix element $\langle \frac{5}{2}^+_1 || E2 || \frac{3}{2}^+_{\rm gs} \rangle$ for ^{29}Na was accomplished according to the relative γ-ray yield between ^{110}Pd and ^{29}Na. Similar approaches have been successfully adopted in other radioactive-ion beam Coulomb-excitation experiments that have also used the isotope separator online technique, e.g. see Ref. [27–30]. The integrated γ-ray yield for the $2^+_1 \rightarrow 0^+_{\rm gs}$ transition in ^{110}Pd was calculated directly using the multiple Coulomb-excitation code GOSIA [31] together with known properties of ^{110}Pd. The calculation was performed based on known matrix elements for all significant couplings up to the second excited 4^+ state in ^{110}Pd [32], then integrating over the energy loss of the beam through the target and over the solid angle subtended by BAMBINO corresponding to acceptance of both scattered-beam ($20.1^\circ - 49.4^\circ$) and recoiling-target ($20.1^\circ - 31.0^\circ$) particles. Corrections for angular distribution effects and internal conversion processes were also taken into account. The total observed number of ^{110}Pd γ rays had two components due to incident-beam isobaric contamination; these were derived according to excitations based on ^{29}Na/^{110}Pd and ^{29}Al/^{110}Pd monopole/quadrupole interactions. The corrected number of counts for this $2^+_1 \rightarrow 0^+_{\rm gs}$ transition in ^{110}Pd was 90(9) for the ^{29}Na/^{110}Pd component, while the number of counts recorded for the $5/2^+_1 \rightarrow 3/2^+_{\rm gs}$ transition in ^{29}Na was 56(7). An experimental Coulomb-excitation cross section for the $5/2^+_1 \rightarrow 3/2^+_{\rm gs}$ transition in ^{29}Na was then deduced relative to the known $2^+_1 \rightarrow 0^+_{\rm gs}$ transition in ^{110}Pd. The unknown ^{29}Na reduced transition matrix element $\langle \frac{5}{2}^+_1 || E2 || \frac{3}{2}^+_{\rm gs} \rangle$ could then be treated as a variable parameter in the GOSIA calculations, while the reduced diagonal matrix element, $\langle \frac{3}{2}^+_{\rm gs} || E2 || \frac{3}{2}^+_{\rm gs} \rangle = 0.121(4)$ eb, was derived from a previous measurement of the ground-state quadrupole moment [17], in order to determine the value consistent with the experimental yield. Effects from virtual excitation to higher-lying states in ^{29}Na were included but found to have negligible impact on the $5/2^+_1 \rightarrow 3/2^+_{\rm gs}$ yield. The yield was also found to be insensitive to sign differences from higher-order couplings, in particular the sign of the diagonal element, $\langle \frac{5}{2}^+_1 || E2 || \frac{5}{2}^+_1 \rangle$, assumed to be $|0.026(1)|$ eb in accordance with a rotational model calculation, only leading to a yield difference at the ~ 0.1 % level depending on constructive or destructive interference modes. Systematics imply that the $5/2^+_1 \rightarrow 3/2^+_{\rm gs}$ transition proceeds largely via an $M1$ decay mode. The estimated $|\langle \frac{5}{2}^+_1 || M1 || \frac{3}{2}^+_{\rm gs} \rangle|$ value of 0.207 μ_N in ^{29}Na was based on previous lifetime measurements in ^{25}Na [33]. The calculated integrated γ-ray yield for the $5/2^+_1 \rightarrow 3/2^+_{\rm gs}$ transition was found to be almost entirely insensitive to the sign and magnitude of the $M1$ matrix element, while a small yield difference of 1.5 % resulted from the angular distribution correction.

A value for $|\langle \frac{5}{2}^+_1 || E2 || \frac{3}{2}^+_{\rm gs} \rangle| = 0.237(21)$ eb has been extracted for ^{29}Na in this work, corresponding to a $B(E2; 5/2^+_1 \rightarrow 3/2^+_{\rm gs}) = 17.7(32)$ W.u. The statistical uncertainty arising from the measured peak areas, ~ 16 %, dominates the quoted 1-σ error on this measurement. Other contributions include uncertainties in the beam composition and target purity, ~ 3 % and < 0.1%

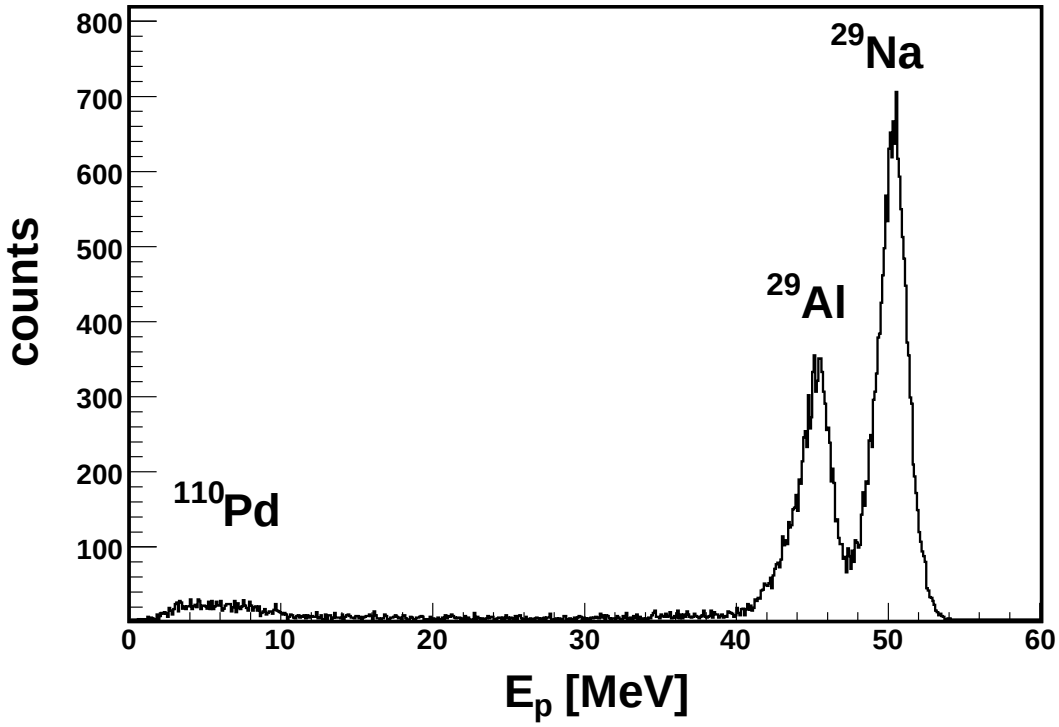

Fig. 2. Particle-energy spectrum corresponding to the total energy deposited in the two innermost annular strips of the BAMBINO silicon array. At high energy the ^{29}Al and ^{29}Na ions can be clearly separated, while the ^{110}Pd ions recoil at much lower energy. The positions of the different particle types are labeled on the spectrum. A linear energy transformation has been applied to the all events registered in the second ring to ensure the centroids corresponding to the different beam particles overlap upon summation.

respectively, along with a $\sim$ 6 % systematic uncertainty in the magnitudes (and signs) of the matrix elements corresponding to couplings with higher-lying states in ^{110}Pd (and ^{29}Na), in addition to the $\sim$ 2 % uncertainty on the relative γ-ray efficiency measurements; all of which are much less significant. As a consistency check cross sections for the $5/2^+_1 \rightarrow 3/2^+_{\rm gs}$ transition in ^{29}Na were also deduced from γ-ray spectra kinematically constrained to events in coincidence with: (i) forward-scattered projectiles (^{29}Na or ^{29}Al); (ii) forward-scattered recoils (^{110}Pd). Experimental cross sections of 155(30) and 61(22) mb were attained for projectile-constrained and recoil-constrained events, respectively. These results are in good agreement with the calculated yield assuming the average value of the above reduced matrix element $\langle \frac{5}{2}^+_1 || E2 || \frac{3}{2}^+_{\rm gs} \rangle$ determined in this measurement: 144 mb for projectile-constrained and 65 mb for recoil-constrained events.

Our experimental result, $|\langle \frac{5}{2}^+_1 || E2 || \frac{3}{2}^+_{\rm gs} \rangle| = 0.237(21)$ eb, is consistent with the prediction of the MCSM using the SDPF-M interaction [20], $|\langle \frac{5}{2}^+_1 || E2 || \frac{3}{2}^+_{\rm gs} \rangle| = 0.232$ eb, which also predicts the correct ground-state spin $I = 3/2^+$ [34] for ^{29}Na (c.f. the result using the USD interaction with $(e_p, e_n) = (1.3e, 0.5e)$:

$I_{\rm gs} = 5/2^+$; $|\langle \frac{3}{2}^+_1 || E2 || \frac{5}{2}^+_{\rm gs} \rangle| = 0.211$ eb). This result therefore supports the theoretical conjecture allowing for neutron excitations across the shell gap, resulting in neutrons filling the next major pf shell before completion of the $N = 20$ sd major shell, and a strongly-mixed state comprising a $30 \sim 40$ % admixture of 2p-2h configurations in the wave function [35]. This scenario would imply a narrow sd-pf neutron-shell gap of ~ 3 MeV [20] for ^{29}Na. Since a successful description of the electromagnetic properties of the $5/2^+_1$ and $3/2^+_{\rm gs}$ states assumes a similar underlying single-particle configuration, it is relevant to discuss the rotational correlations of the significantly enhanced transition probability between these two states. Within the framework of a rotational model calculation and assuming a prolate deformation, an intrinsic quadrupole moment, $Q_t = 0.524(46)$ eb, is deduced from the transition matrix element derived for ^{29}Na from this measurement. This value is in good agreement with the SDPF-M calculation, $Q_t = 0.513$ eb [20]. Contrasting behaviour in the static and dynamic-nuclear properties of ^{29}Na, arising from differences in the underlying single-particle configurations of the ground and excited states, may explain the difference between the present measurement and that of an earlier experimental result using β-NMR spectroscopy, $Q_0 = 0.430(15)$ eb [17]. This intrinsic quadrupole moment, derived from the ground-state spectroscopic quadrupole moment, 0.086(3) eb, also compares well with the SDPF-M calculation, $Q_0 = 0.455$ eb.

In summary, a successful sub-barrier Coulomb-excitation measurement of a radioactive beam of ^{29}Na ions has been performed at the recently commissioned ISAC-II facility at TRIUMF. From the measured γ-ray yields, the transition probability to the first excited state in this nucleus has been determined for the first time. The extracted result shows strong evidence for sd-pf shell mixing in both the ground and first-excited states in ^{29}Na, in good agreement with the SDPF-M prediction [20]. The inadequacy of the USD description of the ground-state properties of ^{29}Na had already been previously established from the earlier static quadrupole moment measurement [17]. This Letter provides further evidence in support of this scenario from a dynamic measurement of the transition probability to the first excited state in ^{29}Na. While the main part of the island of inversion has been largely explained by theoretical interpretation, the boundary regions remain especially challenging. In the future we will extend our measurements to neighbouring nuclei ^{30}Na and ^{31}Mg in order to further test the predictive capabilities of current shell-model theories. This experiment has demonstrated the ability to perform very successful low-energy ISOL experiments with beam rates as low as only a few hundred particles per second. With the proposed advances for the next generation of γ-ray spectrometers, e.g. AGATA [36] and GRETA [37], an order of magnitude increase in γ-ray detection efficiency will be available, allowing for unparalleled access to the most exotic nuclei with beam rates as low as a few tens per second.

Acknowledgments

This work was supported by the DOE, LLNL Contract DE-AC52-07NA27344, the NSF, the NSERC of Canada, and the STFC of the UK. TRIUMF receives federal funding via a contribution agreement with the NRC of Canada. The considerable effort of the operations staff at TRIUMF is gratefully acknowledged. The authors would also like to thank Prof. B. A. Brown and Dr. D. J. Millener for insightful discussions concerning the shell-model calculations.

References

[1] O. Haxel, J. H. D. Jensen and H. E. Suess, Phys. Rev. 75 (1949) 1766.

[2] M. G. Mayer, Phys. Rev. 75 (1949) 1969.

[3] T. Otsuka *et al.*, Phys. Rev. Lett. 87 (2001) 082502.

[4] T. Otsuka *et al.*, Phys. Rev. Lett. 95 (2005) 232502.

[5] T. Otsuka, T. Suzuki and Y. Utsuno, Nucl. Phys. A805 (2008) 127c.

[6] B. H. Wildenthal and W. Chung, Phys. Rev. C 22 (1980) 2260.

[7] E. K. Warburton, J. A. Becker and B. A. Brown, Phys. Rev. C 41 (1990) 1147.

[8] C. Thibault *et al.*, Phys. Rev. C 12 (1975) 644.

[9] X. Campi, H. Flocard, A. K. Kerman and S. Koonin, Nucl. Phys. A251 (1975) 193.

[10] C. Détraz *et al.*, Nucl. Phys. A394 (1983) 378.

[11] C. Détraz *et al.*, Phys. Rev. C 19 (1979) 164.

[12] A. Watt, R. P. Singhal, M. H. Storm and R. R. Whitehead, J. Phys. G 7 (1981) L145.

[13] B. A. Brown and B. H. Wildenthal, Annu. Rev. Nucl. Part. Sci. 38 (1988) 29.

[14] V. Tripathi *et al.*, Phys. Rev. Lett. 94 (2005) 162501.

[15] V. Tripathi *et al.*, Phys. Rev. C 73 (2006) 054303.

[16] B. H. Wildenthal, M. S. Curtin and B. A. Brown, Phys. Rev. C 28 (1983) 1343.

[17] M. Keim *et al.*, Eur. Phys. J. A 8 (2000) 31.

[18] B. V. Pritychenko *et al.*, Phys. Rev. C 66 (2002) 024325.

[19] S. Ettenauer *et al.*, Phys. Rev. C 78 (2008) 017302.

[20] Y. Utsuno *et al.*, Phys. Rev. C 70 (2004) 044307.

[21] Y. Utsuno, T. Otsuka, T. Mizusaki and M. Honma, Phys. Rev C 60 (1999) 054315.

[22] B. A. Brown, Prog. Part. Nucl. Phys. 47 (2001) 517.

[23] R. E. Laxdal, Nucl. Instrum. Methods Phys. Res., Sect. B 204 (2003) 400.

[24] R. E. Laxdal *et al.*, Proc. EPAC2006, Edinburgh, Scotland (2006).

[25] H. C. Scraggs *et al.*, Nucl. Instrum. Methods Phys. Res., Sect. A 543 (2005) 431.

[26] D. Cline, Ann. Rev. Nucl. Part. Sci. 36 (1986) 683.

[27] A. M. Hurst *et al.*, Phys. Rev. Lett. 98 (2007) 072501.

[28] O. Niedermaier *et al.*, Phys. Rev. Lett. 94 (2005) 172501.

[29] I. Stefanescu *et al.*, Phys. Rev. Lett. 98 (2007) 122701.

[30] J. Cederkäll *et al.*, Phys. Rev. Lett. 98 (2007) 172501.

[31] T. Czosnyka, D. Cline and C. Y. Wu, Bull. Am. Phys. Soc. 28 (1983) 745.

[32] L. Hasselgren and D. Cline, "Interacting Bose-Fermi Systems in Nuclei", Ed. F. Iachello, Plenum Press, Ettore Majorana International Science Series 10 (1980) 59.

[33] R. L. Kozub *et al.*, Nucl. Phys. A403 (1983) 155.

[34] G. Huber *et al.*, Phys. Rev. C 18 (1978) 2342.

[35] V. Tripathi *et al.*, Phys. Rev. C 76 (2007) 021301(R).

[36] J. Simpson, J. Phys. G: Nucl. Part. Phys. 31 (2005) S1801.

[37] I. Y. Lee, AIP Conf. Proc. 656 (2003) 343.